Eur. Phys. J. B **54**, 73–81 (2006)
DOI: 10.1140/epjb/e2006-00431-3

THE EUROPEAN PHYSICAL JOURNAL B

# Ground states of an extended Falicov-Kimball model

P.M.R. Brydon[1], M. Gulácsi[2], and A. Bussmann-Holder[1,a]

[1] Max-Planck-Institut für Festkörporforschung, Heisenbergstr. 1, 70569 Stuttgart, Germany
[2] Department of Theoretical Physics, Institute of Advanced Studies, The Australian National University, Canberra, ACT 0200, Australia

Received 12 July 2006
Published online 8 December 2006 – 

**Abstract.** We present a non-perturbative study of an extended Falicov-Kimball model in one dimension. Working within the binary alloy interpretation, we include the spin of the itinerant electrons and a Hubbard interaction to model the inter-electron correlations. We derive an effective Ising model for the atomic configuration in order to show how the Hubbard term affects the stability of the phase separated states. Furthermore, we investigate the competition between the Mott insulator state of the itinerant electrons and the checkerboard phase of the spinless Falicov-Kimball model.

**PACS.** 71.10.Fd Lattice fermion models (Hubbard model, etc.) – 71.30.+h Metal-insulator transitions and other electronic transitions

## 1 Introduction

Although originally introduced as a model of valence transitions [1], the Falicov-Kimball Model (FKM) is today mostly studied as a model for the formation of ordered states in a binary alloy $A_{1-x}B_x$ due to the scattering of itinerant ($c$) electrons off the atomic configuration [2]. The spin of the $c$ electrons is, however, usually ignored as only the charge order is of interest. Furthermore, it is assumed that the only relevant correlations in the system are between the $c$ electrons and the atoms. Although this highly idealized model contains the basic ingredients of a microscopic model of a binary alloy [3], it is, however, insufficient to properly describe the situation in a real solid, where the $c$-electron correlations play a significant role. For this reason, we study here an extended version of the FKM where spin and correlations between the $c$ electrons are included.

The Hamiltonian for this one-dimensional (1D) extended FKM (EFKM) is written

$$\mathcal{H} = -t\sum_{j,\sigma}\left\{c^{\dagger}_{j,\sigma}c_{j+1,\sigma} + \text{H.c.}\right\} + G\sum_{j,\sigma}W(x_j)n^c_{j,\sigma} + U\sum_j n^c_{j,\uparrow}n^c_{j,\downarrow}. \quad (1)$$

Here $t > 0$ is the $c$-electron hopping, $U$ is the Hubbard repulsion between the $c$ electrons, $G = \epsilon_B - \epsilon_A$ is the difference between the single-particle energies of the A and B atoms and $W(x_j)$ is a potential which is 1 (0) on B-atom (A-atom) sites. Deformations of the lattice due to differing atomic radii of the A and B atoms are ignored. The concentration of the two atomic constituents is fixed at $1-x$ and $x$ for the A and B atoms, respectively. The itinerant conduction electron concentration is $n^c$. We work throughout at $T = 0$.

The configuration of the atoms, $W(x_j)$, is chosen to minimize the energy of the $c$ electrons. In the spinless case, a wide variety of different atomic configurations have been obtained. In the $G \to \infty$ limit the A and B atoms adopt either a periodic arrangement (the crystalline state) or segregate to occupy different macroscopic regions of the lattice [2,4]. At weak-coupling, perturbation theory shows that the ground state configuration is either a crystalline state (in analogy to a Peierls instability) or a phase-separated state where the homogeneous and crystalline states or two different crystalline states coexist [5,6]. Numerical studies have revealed that at intermediate coupling a complicated phase diagram results, where segregated (SEG), crystalline and phase-separated states are possible [7,8]. Interestingly, it is found that the behaviour of the model in higher dimensions is qualitatively very similar to the 1D case (i.e. away from half-filling there is a competition between charge order and phase separation) [9].

Until now, most of the work on the various extensions of the FKM has focused on the spinless model [10–13]. Recently, however, there has been increasing interest in the inclusion of spin. This has been most comprehensively studied in the $D \to \infty$ limit, although mainly in

[a] e-mail: a.bussmann-holder@fkf.mpg.de

the interpretation of the FKM as a model for valence-transition systems [14,15]. More closely related to the physics of binary alloys is the possible coexistence of spin and charge order, although this requires that one of the atomic species is magnetically active [16,17]. In both cases, it is found that charge-ordering persists when the $c$ electrons have spin, but the influence of correlations between the $c$ electrons remains to be fully investigated [17].

In this work, we extend our previous study of the spinless FKM to the Hamiltonian described by equation (1) [13,18]. The non-perturbative bosonization method is generalized in order to discuss in detail the effect of the Hubbard interaction on the formation of the SEG phase. We find that attractive (repulsive) interactions lower (raise) the critical coupling for the SEG phase to be realized. This is understood in terms of the change in the charge compressibility of the $c$ electrons due to the interactions. Furthermore, the competition between the Mott insulator state of the Hubbard model and the charge-ordered phases of the FKM is considered. We demonstrate that for a crystalline atomic configuration the EFKM is closely related to the ionic Hubbard model, indicating the presence of a novel dielectric insulator phase [19,20].

## 2 Bosonization

The bosonization technique has been used for many years to study the critical properties of one-dimensional many-electron systems [21]. The bosonization of a tight-binding Hamiltonian is often performed in the continuum limit where the lattice spacing $a \to 0$; this approach fails when interactions with localized states are present. It has recently been demonstrated that the conventional bosonization scheme can be modified for the itinerant electrons in the FKM to account for the interaction with the localized states [13,18]. This is achieved by assuming a finite cut-off $\alpha > a$ on the wavelength of the bosonic density fluctuations [22].

The basic bosonic objects in the theory are the coherent particle-hole excitations about the right and left Fermi points

$$\rho_{\nu,\sigma}(q) = \sum_{0<\nu k'<\pi/a} c^{\dagger}_{k'-q,\sigma} c_{k',\sigma}. \tag{2}$$

The chiral species is denoted by $\nu = R(+),\ L(-)$ as subscript (otherwise). For a system of size $L \gg a$ the $\rho_{\nu,\sigma}(q)$ obey the standard commutation relations

$$[\rho_{\nu,\sigma}(q), \rho_{\nu',\sigma'}(q')]_- = \delta_{\nu,\nu'}\delta_{\sigma,\sigma'}\delta_{q,-q'}\frac{\nu q L}{2\pi} \tag{3}$$

for wave vectors $|q| < \frac{\pi}{\alpha}$. For sufficiently small interactions, the density operators generate the entire state space of the linearized fermion Hamiltonian. It is, however, more convenient to discuss the Bose representation in terms of the dual Bose fields

$$\phi_\sigma(x_j) = -i\sum_\nu \sum_{q\neq 0} \frac{\pi}{qL}\rho_{\nu,\sigma}(q)\Lambda_\alpha(q)e^{iqx_j} \tag{4}$$

$$\theta_\sigma(x_j) = i\sum_\nu \sum_{q\neq 0} \nu\frac{\pi}{qL}\rho_{\nu,\sigma}(q)\Lambda_\alpha(q)e^{iqx_j}. \tag{5}$$

The Bose fields are physically interpreted as potentials: $\partial_x\phi_\sigma(x_j)$ and $\partial_x\theta_\sigma(x_j)$ are, respectively, proportional to the deviation from the noninteracting values of the average spin-$\sigma$ electron and current density at $x_j$. It is convenient to divide the bosonic representation into charge- and spin-sectors, defined by the linear combinations

$$\phi_c(x_j) = \frac{1}{\sqrt{2}}[\phi_\uparrow(x_j) + \phi_\downarrow(x_j)] \tag{6}$$

$$\phi_s(x_j) = \frac{1}{\sqrt{2}}[\phi_\uparrow(x_j) - \phi_\downarrow(x_j)] \tag{7}$$

and similarly for the $\theta$-fields. $\partial_x\phi_c(x_j)$ is proportional to the charge density and $\partial_x\phi_s(x_j)$ is proportional to the spin density of the conduction electrons at $x_j$.

The restriction to density fluctuations with wave vectors $|q| < \frac{\pi}{\alpha}$ is enforced in equations (4) and (5) by the cut-off function $\Lambda_\alpha(q)$. The cut-off function monotonically decreases from unity at $q = 0$ to zero at the Brillouin zone boundaries, with a characteristic decay constant of $\mathcal{O}(1/\alpha)$. The continuous variation of $\Lambda_\alpha(q)$ reflects the gradual crossover of the character of the density fluctuations from long-range bosonic to short-range fermionic. Because the cut-off function excludes density fluctuations with wavelengths $<\mathcal{O}(\alpha)$ from the definition of the Bose fields, the bosonic description effectively assumes that the electrons are delocalized over a characteristic length $\sim\alpha$. This is reflected in the "smearing" of the Bose field commutators

$$[\phi_\eta(x_j), \theta_{\eta'}(x_{j'})]_- = \frac{i\pi}{2}\delta_{\eta,\eta'}\mathrm{sgn}_\alpha(x_{j'} - x_j) \tag{8}$$

$$[\partial_x\phi_\eta(x_j), \theta_{\eta'}(x_{j'})]_- = -i\pi\delta_{\eta,\eta'}\delta_\alpha(x_{j'} - x_j) \tag{9}$$

where the index $\eta = c,\ s$. $\mathrm{sgn}_\alpha(x)$ and $\delta_\alpha(x)$ are the $\alpha$-smeared sign and Dirac delta functions, respectively. The precise form of these functions depends upon $\Lambda_\alpha(q)$ through the definitions

$$\delta_\alpha(x) = \sum_{q\neq 0}\frac{1}{L}\Lambda^2_\alpha(q)\cos(qx) \tag{10}$$

$$\mathrm{sgn}_\alpha(x) = \sum_{q\neq 0}\frac{1}{2qL}\Lambda^2_\alpha(q)\sin(qx) \tag{11}$$

where the sums extend over the first Brillouin zone.

To describe the low-energy physics the $c$-electron dispersion at the two Fermi points is assumed to be linear. Correspondingly, we decompose the $j$-site annihilation operator in terms of states in the vicinity of $k_F$ (the right-moving fields) and $-k_F$ (the left-moving fields):

$$c_{j,\sigma} \approx c_{R,j,\sigma}e^{ik_Fx_j} + c_{L,j,\sigma}e^{-ik_Fx_j}.$$

A Bose representation for the slowly-varying $c_{\nu,j,\sigma}$ may be derived by requiring that it correctly reproduces the fermion anticommutators and noninteracting expectation

values. This is the so-called Mandelstam identity

$$c_{\nu,j,\sigma} = \sqrt{\frac{Aa}{\alpha}}\hat{\chi}_{\nu,\sigma}\exp\left(-\frac{i\nu}{\sqrt{2}}\left[\phi_c(x_j) + \sigma\phi_s(x_j) - \nu\theta_c(x_j) - \nu\sigma\theta_s(x_j)\right]\right). \quad (12)$$

This identity is rigorously valid only in the long-wavelength limit: because of the wavelength cut-off in the definition of the Bose fields, equation (12) may not correctly reproduce the short-range [$<\mathcal{O}(\alpha)$] properties of the $c_{\nu,j,\sigma}$. The dimensionless parameter $A$ is a normalization constant which depends on the cut-off function. The Klein factors $\hat{\chi}_{\nu,\sigma}$ are Majorana fermions, and obey the relation

$$\left[\hat{\chi}_{\nu,\sigma}, \hat{\chi}_{\nu',\sigma'}\right]_+ = 2\delta_{\nu,\nu'}\delta_{\sigma,\sigma'}. \quad (13)$$

The Klein factors $\hat{\chi}_{\nu,\sigma}$ commute with the Bose fields. They are present in order to guarantee the correct accounting of signs in different fermionic operators [21].

An important identity is the representation for the normal-ordered $c$-electron number operator:

$$:n^c_{j,\sigma}: = -\frac{a}{\pi}\partial_x\phi_\sigma(x_j) + \frac{Aa}{\alpha}\sum_\nu \hat{\chi}_{\nu,\sigma}\hat{\chi}_{-\nu,\sigma}e^{i\sqrt{2}\nu[\phi_c(x_j)+\sigma\phi_s(x_j)]}e^{-i2\nu k_F x_j}. \quad (14)$$

The first term on the RHS gives the deviation of the $c$-electron density from its homogeneous non-interacting value and is entirely due to forward scattering ($\nu \to \nu$ processes); the second term is the first order backscattering ($\nu \to -\nu$ processes) correction.

### 2.1 The Hamiltonian in Boson form

The bosonization of the Hamiltonian is accomplished by inserting the relevant bosonization identities. The following analysis is, however, simplified by first expressing the atomic species at each site in terms of pseudospin-$\frac{1}{2}$ operators, $W(j) - \frac{1}{2} = \tau^z_j$. In the pseudospin representation, spin-$\uparrow$ at site $j$ indicates an A-atom and spin-$\downarrow$ a B-atom. The fixed concentration of the atomic constituents implies a constant pseudospin magnetization $m^z = \frac{1}{2} - x$. The electron-atom interaction is then re-written

$$G\sum_{j,\sigma} W(x_j)n^c_{j,\sigma} = G\sum_{j,\sigma}\tau^z_j :n^c_{j,\sigma}: + GNn^c m^z. \quad (15)$$

Since the last term on the right hand side is a constant which does not contribute to the physics it will be neglected in the following. Substituting equation (14) into equation (15) and using the bosonization identities, we obtain the bosonized Hamiltonian

$$\begin{aligned}\mathcal{H} = &\sum_{\eta=c,s}\frac{v_\eta a}{2\pi}\sum_j\left\{\frac{1}{K_\eta}\left(\partial_x\phi_\eta(x_j)\right)^2 + K_\eta\left(\partial_x\theta_\eta(x_j)\right)^2\right\} \\ &- 2U\frac{A^2a^2}{\alpha^2}\sum_j\cos[2\sqrt{2}\phi_c(x_j) - 4k_F x_j] \\ &+ 2U\frac{A^2a^2}{\alpha^2}\sum_j\cos[2\sqrt{2}\phi_s(x_j)] \\ &- \frac{\sqrt{2}Ga}{\pi}\sum_j\tau^z_j\partial_x\phi_c(x_j) - 4G\frac{Aa}{\alpha}\sum_j\tau^z_j\cos[\sqrt{2}\phi_s(x_j)] \\ &\times\sin[\sqrt{2}\phi_c(x_j) - 2k_F x_j]. \end{aligned} \quad (16)$$

Since the Klein factor products commute with the Hamiltonian, they have been replaced by their eigenvalues $\hat{\chi}_{R\sigma}\hat{\chi}_{L\sigma} = \langle\hat{\chi}_{R\sigma}\hat{\chi}_{L\sigma}\rangle = -i$. This choice gives the standard sign of the Umklapp and backscattering terms. Note that the sign of the $2k_F$-backscattering off the pseudospins is unimportant, as this term acts like a hybridization between the left- and right-moving fermions, hence only its absolute value is significant.

The first term on the RHS of equation (16) describes the forward-scattering interactions between the $c$ electrons. The separation of charge and spin is clear, with different charge and spin velocities $v_\eta$ and Luttinger parameters $K_\eta$, $\eta = c, s$. In the limit $Ua/v_F \ll 1$, these can be expressed in the analytical forms

$$K_c = \frac{1}{\sqrt{1+\frac{Ua}{\pi v_F}}}, \qquad v_c = \frac{v_F}{K_c} \quad (17)$$

$$K_s = \frac{1}{\sqrt{1-\frac{Ua}{\pi v_F}}}, \qquad v_s = \frac{v_F}{K_s}. \quad (18)$$

The Fermi velocity is defined $v_F = -2ta\sin(k_F a)$ where $k_F = \pi n^c/a$. By rescaling the spin and charge fields

$$\widetilde{\phi}_\eta(x_j) = \frac{1}{\sqrt{K_\eta}}\phi_\eta(x_j), \qquad \widetilde{\theta}_\eta(x_j) = \sqrt{K_\eta}\theta_\eta(x_j) \quad (19)$$

the first term on the RHS of equation (16) is converted into the standard non-interacting Bose field Hamiltonian [21]. The second term of equation (16) describes the Umklapp scattering of the $c$ electrons, while the third term is due to the inter-electron backscattering. The fifth and sixth terms are the forward-scattering and $2k_F$-backscattering interactions of the $c$ electrons with the pseudospins.

## 3 The canonical transform

The phase diagram of the spinless FKM reveals a competition between crystalline order and the SEG phase [8,13,18]. The crystalline order originates from the backscattering of the $c$ electrons off the atomic configuration. For a periodic atomic configuration with wavevector $2k_F$, the backscattering term hybridizes the left- and

right-moving electrons, thus opening a gap in the $c$ electron spectrum and lowering the total electronic energy. This competes with the tendency to segregate; the effective segregating interaction, however, is not clearly seen in equation (16). It can be presented in a more obvious way by a canonical transformation which removes the forward-scattering interaction. We generalize the transformation used in the analysis of the spinless FKM to our extended model:

$$\hat{U} = \exp\left\{ i\frac{\sqrt{2K_c}Ga}{\pi v_c}\sum_{j'} \tau_j^z \widetilde{\theta}_c(x_{j'}) \right\}. \tag{20}$$

Using the Baker-Hausdorff formula the canonical transformation of the Hamiltonian is carried out to all orders. The transformed Bose operators are written

$$\hat{U}^\dagger \widetilde{\phi}_c(x_j)\hat{U} = \widetilde{\phi}_c(x_j) - \frac{\sqrt{K_c}Ga}{\sqrt{2}v_c}\sum_{j'} \tau_{j'}^z \mathrm{sgn}_\alpha(x_{j'} - x_j) \tag{21}$$

$$\hat{U}^\dagger \partial_x\widetilde{\phi}_c(x_j)\hat{U} = \partial_x\widetilde{\phi}_c(x_j) + \frac{\sqrt{2K_c}Ga}{v_c}\sum_{j'} \tau_{j'}^z \delta_\alpha(x_j - x_{j'}). \tag{22}$$

All other operators are invariant under the transformation. In particular, the spin fields and pseudospin operators are unchanged: i.e., the atomic configuration and also the magnetic properties of the $c$ electrons are maintained.

By substituting the transformed Bose fields [Eqs. (21) and (22)] into equation (16) we obtain the Hamiltonian

$$\begin{aligned}\hat{U}^\dagger \mathcal{H}\hat{U} = &\sum_{\eta=c,s}\frac{v_\eta a}{2\pi}\sum_j \left\{ \left(\partial_x\widetilde{\phi}_\eta(x_j)\right)^2 + \left(\partial_x\widetilde{\theta}_\eta(x_j)\right)^2 \right\} \\ &+2U\frac{A^2a^2}{\alpha^2}\sum_j \cos\left[2\sqrt{2K_s}\widetilde{\phi}_s(x_j)\right] \\ &-2U\frac{A^2a^2}{\alpha^2}\sum_j \cos\left[2\sqrt{2K_c}\widetilde{\phi}_c(x_j) - 2\mathcal{K}(x_j)\right. \\ &\left.-4k_F x_j\right] - \frac{K_c G^2 a^2}{\pi v_c}\sum_{j,j'} \tau_j^z \delta_\alpha(x_j - x_{j'})\tau_{j'}^z \\ &-4G\frac{Aa}{\alpha}\sum_j \tau_j^z \cos\left[\sqrt{2K_s}\widetilde{\phi}_s(x_j)\right] \\ &\times \sin\left[\sqrt{2K_c}\widetilde{\phi}_c(x_j) - \mathcal{K}(x_j) - 2k_F x_j\right] \end{aligned} \tag{23}$$

where

$$\mathcal{K}(x_j) = \frac{K_c Ga}{v_c}\sum_{j'} \tau_{j'}^z \mathrm{sgn}_\alpha(x_{j'} - x_j). \tag{24}$$

Since the expressions for the transformed charge fields are exact, it follows that equation (23) is equivalent to equation (16). The only difference is that the basis has been rotated to give an explicit representation of the effective interactions between the pseudospins, i.e. the Ising term on the third line.

This Ising term originates from the removal of the forward-scattering coupling between the $c$ electrons and the pseudospins. It is clear from equation (1) that the electron-atom interaction favours $c$-electron occupation of A-atom sites and disfavours occupation of B-atom sites. Because of the finite spread of the $c$-electron wavefunctions, this repulsion is spread over a characteristic length scale $\sim\alpha$. This is apparent in equation (23) where $\alpha$ sets the range of the effective interaction potential $\delta_\alpha(x)$ in the Ising term. This potential is the same $\alpha$-smeared $\delta$-function as for the Bose field commutator. For any reasonable choice of cut-off function, the potential $\delta_\alpha(x)$ is positive for $|x| < \alpha$ and decreases rapidly with increasing distance. For example, for the following two cut-off functions

$$\Lambda_\alpha(q) = \begin{cases} \exp(-\alpha|k|/2\pi) & \text{Exponential} \\ \exp(-\alpha^2k^2/2\pi^2) & \text{Gaussian} \end{cases} \tag{25}$$

the corresponding interaction potential is given by

$$\delta_\alpha(x) = \begin{cases} \alpha/(\alpha^2 + \pi^2x^2) & \text{Exponential} \\ (\sqrt{\pi}/2\alpha)\exp(-\pi^2x^2/4\alpha^2) & \text{Gaussian.} \end{cases} \tag{26}$$

Despite its importance to our analysis, it is not possible to determine the exact range of the potential $\alpha$ within the bosonization scheme. Although a quantitative estimate is in general difficult, in the limit $n^c \ll 1$ the individual behaviour of the $c$ electrons in the FKM may be well approximated by the problem of a quantum particle in a potential with two values $\pm G/2$ [18,24]. Solving the associated Schrodinger equation for the low-energy ($E = 0$) states, for particles moving in a region with potential $-G/2$ (sites occupied by A atoms) the wavefunctions are plane waves; for regions where the potential is $G/2$ (sites occupied by B atoms) the wavefunctions decay exponentially on a length scale $\xi \sim G^{-1/2}$. The identification of $\alpha$ with the finite spread of the delocalized $c$-electron wavefunctions implies that $\alpha \sim \xi$, as was previously found in a similar bosonization study of the Kondo lattice model [22]. We therefore use in the following the approximation $\alpha = bG^{-1/2}$ where $b$ is a constant to be determined.

Because the Ising interaction potential $\delta_\alpha(x)$ is positive for $x < \alpha$ and decreases rapidly with increasing distance, the Ising term describes ferromagnetic interactions between the pseudospins, i.e. the Ising term favours the clustering or segregation of alike atoms. The structure and interpretation of this interaction is identical to that in the spinless case; the magnitude of this term is, however, increased by a factor of $2K_c v_F/v_c = 2K_c^2$. While the factor of two is due to the extra degree of freedom from the spins, the presence of $K_c$ is a consequence of the change in the charge compressibility in the interacting system. For a Tomonaga-Luttinger liquid, the compressibility is given by $\kappa = \kappa_0 K^2$, where $\kappa_0$ is the charge compressibility in the non-interacting system. Repulsive interactions ($K < 1$) therefore decrease the compressibility, whereas attractive interactions ($K > 1$) increase it. In the SEG phase, the $c$ electrons tend to stay within the A atom cluster, enhancing their density: a reduced (enhanced) charge

compressibility will therefore resist (support) the formation of the SEG phase.

## 4 The phase diagram

From the transformed Hamiltonian an effective model for the pseudospins can be derived by replacing the charge and spin fields by their expectation values in the $2k_F$-backscattering interaction with the pseudospins [18]:

$$\mathcal{H}_{\rm eff} = -\frac{K_c G^2 a^2}{\pi v_c}\sum_{j,j'}\tau_j^z\delta_\alpha(x_j - x_{j'})\tau_{j'}^z - 4G\frac{Aa}{\alpha}\sum_j \tau_j^z \cos\left[\sqrt{2K_s}\langle\widetilde{\phi}_s\rangle\right]\sin\left[\sqrt{2K_c}\langle\widetilde{\phi}_c\rangle - \langle\mathcal{K}(x_j)\rangle - 2k_F x_j\right]. \quad (27)$$

Here also $\mathcal{K}(x_j)$ is replaced by its expectation value, as it is a constant of motion. $\mathcal{K}(x_j)$ displays very different behaviours in the crystalline and the SEG states. Referring to equation (24) we may interpret $\mathcal{K}(x_j)$ as subtracting the magnetization of the pseudospins more than $\alpha$ to the right of site $j$ from the magnetization of the pseudospins more than $\alpha$ to the left of site $j$: this quantity vanishes for an infinite chain in a crystalline phase. Therefore, in the crystalline phase only the mean value of $\langle\widetilde{\phi}_c\rangle$ has to be chosen to minimize the backscattering energy.

For the SEG phase, in contrast, the different magnetization of the pseudospins in the A- and B-atom fractions of the lattice produce a linear dependence of $\mathcal{K}(x_j)$ on $x_j$. Assuming that the B-atom fraction resides to the left of site $j'$ and the A-atom fraction is located to the right of site $j'$, we obtain $\mathcal{K}(x_j) \approx (K_c G a/v_c)|j' - j|$ [18]. Since the SEG phase does not produce a gap in the $c$-electron spectrum, the expectation values of the $\widetilde{\phi}_{c,s}$ fields are determined by the Hubbard interaction.

### 4.1 Segregation

The effective Hamiltonian equation (27) can be used to the derive the critical Coulomb repulsion for the SEG phase. We first restrict the range of the Ising interaction to nearest-neighbours only

$$-\frac{K_c G^2 a^2}{\pi v_c}\sum_{j,j'}\tau_j^z\delta_\alpha(x_j - x_{j'})\tau_{j'}^z \approx -\frac{2K_c G^2 a^2}{\pi v_c}\delta_\alpha(a)\sum_j \tau_j^z\tau_{j+1}^z. \quad (28)$$

Since the potential $\delta_\alpha(x)$ falls off rapidly with increasing distance (see Sect. 3), this truncation should not significantly affect the stability of the SEG phase. Making the appropriate replacements for the Bose fields and $\mathcal{K}(x_j)$, we obtain an effective Hamiltonian in the form of a quasiperiodic Ising model (QPIM):

$$\mathcal{H}_{\rm eff} = -\mathcal{J}\sum_j \tau_j^z\tau_{j+1}^z + h\sum_j \tau_j^z\cos(\omega j + \phi). \quad (29)$$

In equation (29) $\mathcal{J} = K_c G^2 a^2 \delta_\alpha(a)/\pi v_c$, $h = -(4GAa/\alpha)\cos(\sqrt{2K_s}\langle\widetilde{\phi}_s\rangle)$, $\omega = \omega_\pm \approx \pi n^c \pm K_c G a/v_c$ (the two values $\omega_+$ and $\omega_-$ are realized in the different sections of the segregated lattice) and $\phi$ is a constant. In general, $\omega_\pm/\pi$ are irrational numbers.

The QPIM has been studied by Sire for constant $\omega$ [25]. The phase diagram of the model exhibits a competition between ferromagnetic order due to the Ising interaction, and the so-called adiabatic order due to the antialignment with respect to the magnetic field. The ferromagnetic phase is stable for $\mathcal{J} > \mathcal{J}_{c1} = h/\sin(1/2\omega)$, while the adiabatic phase is found at couplings $\mathcal{J} < \mathcal{J}_{c2} = h\sin(1/2\eta\omega)\sin(1/2[\eta+1]\omega)/\sin(1/2\omega)$, where $\eta$ is the largest integer smaller than $\pi/\omega$. For intermediate couplings $\mathcal{J}_{c2} < \mathcal{J} < \mathcal{J}_{c1}$, a quasiperiodic arrangement of adiabatically- and ferromagnetically-ordered clusters is found. The weak-coupling adiabatic and strong-coupling ferromagnetic phases correspond to the crystalline and SEG phases, respectively, but there is no direct analogue of the QPIM's intermediate phase. Although the work in [25] was performed in the grand canonical ensemble, it is possible to apply the results to the Hamiltonian equation (29) with a fixed magnetization for the pseudospins. In particular, the critical coupling $\mathcal{J}_{c1}$ for ferromagnetism can be used to obtain the critical coupling for the appearance of the SEG phase, as it was derived from general arguments which remain valid in the canonical ensemble. Inserting the values of the coupling constants in equation (29) into the definition of $\mathcal{J}_{c1}$ the critical coupling $G_c$ is given by

$$\frac{G_c a}{v_F}K_c^2\sin(\tfrac{1}{2}[\pi n^c + K_c^2 G_c a/v_F]) = \frac{2A\pi}{\alpha\delta_\alpha(a)}|\sin(\sqrt{2K_s}\langle\widetilde{\phi}_s\rangle)|. \quad (30)$$

Note that we have chosen $\omega = \omega_+$ to control the critical coupling as this gives the correct monotonic dependence of $G_c$ upon the filling in the spinless case [5,8].

#### 4.1.1 U = 0

We first consider the case $U = 0$ which was partially addressed in [18]. In the absence of interactions between the $c$ electrons $K_c = 1$ and the field $\widetilde{\phi}_s$ in equation (30) is replaced by its non-interacting expectation value, $\langle\widetilde{\phi}_s\rangle = 0$. The effective Hamiltonian equation (27) is then the same, up to a factor of two, as the one for the spinless model [18]. It follows that the critical coupling for segregation in our model with B-atom concentration $x$ and $c$-electron concentration $n^c$ is *identical* to the critical coupling in the spinless model with B-atom concentration $x$ and $c$-electron

concentration $n^c/2$. For the case $x = n^c/2$ the critical coupling is given by

$$G_{c0}/t = \frac{0.5\sin(n^c\pi/2)}{1-\sin(n^c\pi/2)}. \quad (31)$$

This is illustrated in Figure 1 as the dashed blue line. The blue circles are the numerical results for the critical coupling in the spinless FKM obtained by Gajek et al. [8].

The relationship between the phase diagram of the spinless FKM and the $U = 0$ limit of the EFKM can be made more precise. Considering equation (1) it is noted that when $U = 0$ the density of spin $\sigma$ electrons at site $j$ depends only on the atomic configuration and *not* on the density of the spin $-\sigma$ electrons. Consequently, the atomic configuration that minimizes the energy of one electron spin-component also minimizes the total energy of the conduction electrons. Minimizing the energy of a single spin-component with respect to the atomic configuration is effectively identical to the spinless FKM. This means that for B-atom and conduction electron concentrations $x$ and $n^c$, respectively, the ground state atomic configuration of the EFKM is *always* identical to that in the FKM with B-atom and conduction electron concentrations $x$ and $n^c/2$ and the same value of the coupling $G$.

This explains the differences between the phase diagrams of the spinless FKM and EFKM along the line $x + n^c = 1$ [26]. In the former case, the system is at half-filling, which for sufficiently large $G$ always exhibits a crystalline configuration [4]. In the latter case, crystalline, phase-separated and segregated states are all found for $x + n^c = 1$. The mapping of the EFKM onto the spinless FKM indicates that the condition $x + n^c = 1$ for the EFKM is only ever equivalent to a half-filling state in the spinless FKM for $x = 1$. For all other values of $x$, the system maps onto the spinless FKM below half-filling. It is thus not surprising to obtain phase-separation in the EFKM for $x + n^c = 1$ and $x < 1$.

Most work on the EFKM has been performed to model valence-transitions where charge-transfer between the conduction electrons and localized orbitals takes place [14]. In this case, the limitation of each localized orbital to single occupation prevents a direct mapping onto the phase diagram of the spinless FKM. In particular, consider the "half-filling" case $x + n^c/2 = 1$. If the localized electron energy level is located at the centre of the conduction band in the $G = 0$ system, the localized level and the conduction band are both half-filled. Lowering the energy of the localized level, a charge transfer from the conduction band into the localized orbital takes place. In the spinless case, this "valence change" is only completed when the localized level lies at the bottom of the conduction band; in the EFKM, however, it occurs before the localized level reaches the bottom of the conduction band. The relationship between the spinless and spinful models is thus more complicated than in the binary alloy interpretation.

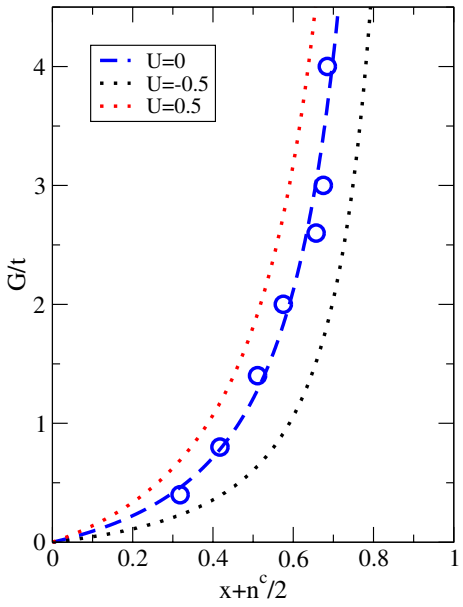


**Fig. 1.** (Color online) Critical line $G_c(n)$ for the formation of the SEG phase. Note that the SEG phase is always realized for $G > G_c$. It is assumed that $x = n^c/2$. In the legend, the value of $U$ is given in units of $\pi v_F/a$. The $U = 0$ curve was originally derived for the spinless model; the expression was derived by fitting to the data points (blue circles) taken from reference [8].

#### 4.1.2 U ≠ 0

For finite $U$ the two cases $U > 0$ (repulsive interactions) and $U < 0$ (attractive interactions) have to be distinguished. For $G = 0$, the former case is at the Tomonaga-Luttinger fixed point for $n^c \neq 1$ and a Mott insulator at $n^c = 1$, i.e. the charge and spin sectors are gapless except at half-filling of the conduction band, where the charge sector develops a gap. The Mott insulator will be discussed in Section 4.2. In the case of repulsive interactions, the system is a Luther-Emery liquid for all fillings, with the spin sector being gapped. The Luther-Emery liquid can be phenomenologically visualized as a system where the on-site singlet-pairing of electrons requires a finite energy for a spin excitation. This pairing does not, however, imply superconductivity as there is a competition with charge-density wave formation, which is derived by comparing the respective susceptibilities [21].

For $n^c < 1$ the charge sector remains gapless for both attractive and repulsive interactions. In the $U = 0$ case the forward-scattering coupling of the charge sector to the pseudospins is found to be principally responsible for the formation of ordered atomic configurations. Although we may expect the charge sector to be similarly important in the $U \neq 0$ case, the renormalization of the $c$-electron properties by the interactions must be taken into account. Note that we continue with the assumption that $x + n^c/2 < 1$.

As outlined above the rescaling of the charge susceptibility changes the magnitude of the segregating interaction (see Sect. 3). To obtain the critical segregation line, however, the effect of the interactions on the spin sector have to be considered. For $U > 0$, $\langle\phi_s\rangle$ can still be replaced

by its non-interacting expectation value in equation (30). In the Luther-Emery liquid, however, the spin-sector is gapped and fluctuations in $\phi_s$ are suppressed, $\phi_s = \langle\phi_s\rangle$. The expectation value is chosen to minimize the backscattering energy [second term on the RHS of equation (23)] which implies $\sqrt{K_s}\langle\phi_s\rangle = \pi(2m-1)/2\sqrt{2}$ where $m$ is an integer. Inserting this result into equation (30) we find that the RHS is the same as in the non-interacting case. Thus, the formation of the Luther-Emery state does not alter the $c$-electron backscattering off the atomic configuration, and hence has no influence on the critical segregation line. This observation underlines the importance of the charge sector for the formation of the SEG phase.

Independent of the sign of $U$ the critical line for segregation is rescaled $G_c \to K_c^2 G_c$, i.e. for $K_c \neq 1$ the critical line is given by $G_{c0}/K_c^2$, where $G_{c0}$ is the critical line for $U = 0$. For the case $x = n^c/2$, the general form of the critical segregating interaction is given by

$$G_c/t = \frac{1}{K_c^2}\left[\frac{0.5\sin(n^c\pi/2)}{1-\sin(n^c\pi/2)}\right]. \tag{32}$$

Using the weak-coupling form of $K_c$ [equation (17)], $G_c$ as a function of $x + n^c/2$ for $U > 0$ and $U < 0$ is shown by the red and black dotted lines in Figure 1. The critical line is robust in the presence of weak interactions between the conduction electrons.

### 4.2 Ordered phases

Until now our analysis of the SEG phase was limited to the case $x + n^c/2 < 1$. Here we consider the appearance of ordered phases in the half-filling limit $x + n^c/2 = 1$. For the corresponding $(x + n^c = 1)$ spinless FKM (i.e. one $c$-electron for each A-atom), a crystalline ground state is always realized for sufficiently large values of $G$. In the special case when $x = n^c = 0.5$, the spinless FKM is in the so-called checkerboard state, where the B atoms occupy one sublattice only. This is known to be the ground state for $G \gg t$ and $G \ll t$ [2,6]; numerical results indicate that it remains the ground state also for intermediate couplings [27,8].

Generalizing the argument of Section 4.1.1, for $U = 0$ the checkerboard state should be realized for all $G$ when $x = 0.5$ and $n^c = 1$. For $U < 0$, the gapping of the spin sector will not affect the stability of this state, as the effective Hamiltonian for the $\tau$ pseudospins is formally the same as in the spinless FKM. When $U > 0$, however, the $G = 0$ limit of equation (1) describes a Mott insulator where the charge sector develops a gap. Phenomenologically, in the Mott insulator one $c$-electron occupies each site and a finite energy is required to produce a charge excitation. In the context of the Hubbard model, this requires the minimization of the Umklapp term by replacing $2\sqrt{2}\phi_c = 0 \pmod{2\pi}$.

The competition between the Mott insulator and the checkerboard phase is reminiscent of the physical situation in the so-called ionic Hubbard model [28,19,29]. This differs from the conventional Hubbard model by the presence of a staggered potential, i.e.

$$\mathcal{H}_{\rm stag} = \Delta\sum_{j\sigma}(-1)^j n^c_{j,\sigma}.$$

The bosonic representation of this potential is given by

$$\mathcal{H}_{\rm stag} = -2\Delta\frac{Aa}{\alpha}\sum_j \cos[\sqrt{2}\phi_s(x_j)]\sin[\sqrt{2}\phi_c(x_j)]. \tag{33}$$

In the semi-classical approximation, the energy of $\mathcal{H}_{\rm stag}$ is minimized by choosing $\sqrt{2}\phi_s = 0 \pmod{2\pi}$, $\sqrt{2}\phi_c = \pi/2 \pmod{2\pi}$ or $\sqrt{2}\phi_s = \pi \pmod{2\pi}$, $\sqrt{2}\phi_c = 3\pi/2 \pmod{2\pi}$. This characterizes a $2k_F$ CDW state and corresponds to a Peierls-like phase [30]. The values of $\phi_c$ which minimize $\mathcal{H}_{\rm stag}$, however, maximize the Umklapp term and vice versa. This implies a competition between the two insulating states, i.e. the Mott insulator with a homogeneous ground state and the Peierls-like state with a CDW-type ordering of the $c$ electrons.

In the limit $\Delta \gg U$, the staggered potential produces the larger gap at the Fermi surface and correspondingly the Peierls-like state is stable. The spin and charge fields adopt the values which minimize $\mathcal{H}_{\rm stag}$. In the opposite limit $\Delta \ll U$, the Mott insulator has the larger gap: the spin sector remains gapless while the charge sector has the value that minimizes the Umklapp scattering energy. At intermediate couplings, however, there is a third dielectric insulator phase, where both the spin and charge sectors are gapped [19,29]. The dielectric insulator exhibits a spontaneous bond dimerization $\Delta_B \neq 0$, defined

$$\Delta_B = \sum_{j,\sigma}(-1)^j\left\langle c^\dagger_{j,\sigma}c_{j+1,\sigma} + \text{H.c.}\right\rangle. \tag{34}$$

Within the dielectric insulator phase $\langle\phi_c\rangle$ takes a value intermediate between that in the Peierls and Mott insulators, indicating the presence of excitations with fractional charge [20]. The spin sector remains gapped as in the Peierls insulator.

The application of the ionic Hubbard model results to the EFKM with $n^c = 1$ and $x = 0.5$ is straightforward: by replacing $\tau^z_j$ by $(1/2)(-1)^j$ (corresponding to the checkerboard state) in equation (16) and neglecting rapidly-fluctuating terms, we obtain a staggered field with $\Delta = G$ which shows that the Peierls state of the ionic Hubbard model is equivalent to the checkerboard state in the EFKM. However, since the atoms adopt the configuration which minimizes the $c$-electron energy, a further mapping requires a stability analysis of the FKM's checkerboard state for all $U$. At present, although we cannot provide a rigorous proof in the general case, it can be argued that the checkerboard state is stable in the limits $U \ll G, t$ and $U \gg G, t$. In the former case, the checkerboard state clearly produces the larger gap at the Fermi energy, and can be expected to be stable.

In the $U \gg t, G$ case the same arguments indicate that a Mott insulator is realized, where the effective

Hamiltonian for the system to leading order in $t/U$ is the spin-$\frac{1}{2}$ Heisenberg model

$$\mathcal{H}_{\text{H}} = \sum_j J_H(j) \left( \mathbf{S}_j \cdot \mathbf{S}_{j+1} - \frac{1}{4} \right) \tag{35}$$

with

$$J_H(j) = \frac{2t^2}{U} \times \begin{cases} U^2/(U^2 - G^2) & W(x_j) \neq W(x_{j+1}) \\ 1 & W(x_j) = W(x_{j+1}). \end{cases} \tag{36}$$

If the checkerboard state is realized, the exchange-coupling is site-independent and $J_H(j) = 2t^2U/(U^2 - G^2) = \widetilde{J}$. For any other atomic configuration, the exchange constant in equation (35) is site-dependent. Although an exact solution of equation (35) is not available, the energy of the checkerboard state ($E = -2\ln(2)\widetilde{J}$) can be compared to two other configurations: the SEG phase and the "two-molecule" state (i.e. a four-site unit cell with B atoms on the first two sites). In the SEG phase, the energy per site is the same [up to $\mathcal{O}(1/N)$] as in the uniform Heisenberg chain with coupling $J_H = 2t^2/U$, and correspondingly the SEG phase has higher energy than the checkerboard state. The two-molecule phase is equivalent to a dimerized Heisenberg chain $J_H(j) = J(1 + (-1)^j\delta)$ with $J = t^2(2U^2 - G^2)/[U(U^2 - G^2)]$ and $\delta = G^2/(2U^2 - G^2)$. Although energetically favourable as compared to the uniform $J_H(j) = J$ state due to the modulation of the exchange, it is higher in energy by $J\delta(2\ln 2 - \gamma\delta^{1/3})$ as compared to checkerboard state, where $\gamma \sim 0.3$ [31]. Other periodic phases can be considered as well but it seems unlikely that these have lower energies: both the exchange-modulation and the average value of the Heisenberg interaction across the lattice will be smaller than in the two molecule state. In the limit $U \gg t, G$ we conclude that the checkerboard state is realized. Since the checkerboard state is stable for $U \gg t, G$ and $U \ll t, G$, it is suggestive to conclude that it remains stable at all values of the Hubbard interaction, and the intermediate dielectric insulator phase appears in the EFKM.

The conclusions for the checkerboard state are also valid for the situation $x + n^c/2 = 1$ with $n^c < 1$. Since the $c$-electron band is not half-filled, a Mott insulator is not realized at any value of $U$ when $G = 0$. However, as has been shown in [32], a generalization of the ionic Hubbard model with scattering off an atomic configuration of periodicity $2k_F < \pi/a$ can induce the Mott insulator phase. In the $U = 0$ limit of the EFKM a periodic state is realized for sufficiently large $G$. The concentration of A atoms is half the concentration of electrons and each A-atom site will tend to be doubly occupied while each B-atom site will tend to have zero occupation. For finite $U > G$, however, the Coulomb penalty for double occupancy will be larger than the energy gain, and the Peierls insulator is unstable. Assuming that the crystalline configuration remains stable, there will be a charge-transfer from the A-atom sites to the B-atom sites to minimize the Coulomb repulsion, thus leading to a Mott-like state. As above, the competition between the Mott and Peierls insulating states leads to an intermediate insulating state. This a generalization of the dielectric insulator, distinguished by a non-vanishing $2k_F$-modulation of the bond operator $\Delta_B(2k_F) = \sum_j \cos(2k_F x_j)\langle c^\dagger_{j,\sigma} c_{j,\sigma} + \text{H.c.}\rangle$. The formation of this state is dependent upon the stability of the crystalline states, which remains to be investigated. It should be noted that although for $U = 0$ the periodic ionic configurations are the ground state in the $G \gg t$ model, in the $G \ll t$ limit not all periodic configurations are stable. Instead, as demonstrated in [6], there is a large range of fillings satisfying $x + n^c/2 = 1$ where the EFKM shows a phase separation between a homogeneous (pure-A or pure-B) and a periodic phase. The stability of these phases in the presence of $U$ remains an open problem.

## 5 Conclusions

In this paper we have generalized a previous analysis of the spinless FKM [13,18] to a model including spin and the Hubbard interaction between the $c$ electrons. Using a generalization of the bosonization technique, the discrete atomic configuration is taken into account. This is achieved by introducing a finite minimum wavelength $\alpha > a$ for the bosonic density fluctuations of the $c$ electrons, which corresponds to a delocalization length scale. The finite spread of the $c$-electron wavefunctions directly leads to the appearance of an effective segregating interaction, which is revealed by the canonical transformation.

Adopting a pseudospin-$\frac{1}{2}$ representation for the atoms, the $c$ electron fields are removed from the canonically transformed Hamiltonian to obtain an effective Ising model for the atomic configuration. For vanishing $U$, this effective model is the same as that derived for the FKM [18], providing a correspondence between the EFKM and the FKM. Using this analogy to define a "half-filling" condition, the effect of the Hubbard term on the position of the critical segregation line was investigated. It was found that only the variation of the charge-sector properties are important for the onset of segregation: enhanced charge compressibility for attractive interactions lowers the critical line, while reduced charge compressibility in the repulsive model increases the minimum coupling for segregation.

We also examined the modifications of the ground states at the EFKM's "half-filling" point, where in the $U = 0$ model the checkerboard phase is realized. For $U > 0$, the checkerboard phase competes with the Mott insulator in a similar way as the Peierls insulating state in the ionic Hubbard model. Using weak-coupling and strong-coupling results, we found that the checkerboard atomic configuration remains stable for $U \ll t, G$ and $U \gg t, G$, suggesting the conclusion that an exotic insulating state is realized in the EFKM. A similar situation might occur for other periodic atomic configurations.

The EFKM is an important step in generalizing the many exactly known results of the spinless model to more realistic systems. A reasonable extension of this work would be to assume that at least one of the atomic species

in the binary alloy carries a magnetic moment, which couples to the conduction electrons via a Kondo interaction. This is expected to lead to an interesting interplay between charge and magnetic order as has been shown for manganites [15]. Alternatively, extensions to include a hybridization between the itinerant and localized orbitals [11,13], or a weak hopping term between nearest-neighbour localized orbitals [12], could be used in describing valence transition physics.

Part of this work was performed within the EU CoMePhS project.

## References


1. L.M. Falicov, J.C. Kimball, Phys. Rev. Lett. **22**, 997 (1969); R. Ramirez, L.M. Falicov, Phys. Rev. B **3**, 2425 (1971)
2. T. Kennedy, E.H. Lieb, Physica A **138**, 320 (1986)
3. F. Ducastelle, *Order and Phase Stability in Alloys* (North-Holland, New York, 1991)
4. P. Lemberger, J. Phys. A: Math. Gen. **25**, 715 (1992)
5. J.K. Freericks, L.M. Falicov, Phys. Rev. B **41**, 2163 (1990)
6. J.K. Freericks, Ch. Gruber, N. Macris, Phys. Rev. B **53**, 16189 (1996).
7. P. Farkašovský, I. Bat'ko, J. Phys.: Cond. Mat. **5**, 7131 (1993)
8. Z. Gajek, J. Jędrzejewski, R. Lemański, Physica A **223**, 175 (1996)
9. J.K. Freericks, Phys. Rev. B **47**, 9263 (1993)
10. Z. Gajek, R. Lemański, Acta. Phys. Pol. B **32**, 3473 (2001)
11. T. Portengen, Th. Östreich, L.J. Sham, Phys. Rev. B **54**, 17452 (1996)
12. C.D. Batista, Phys. Rev. Lett. **89**, 166403 (2002)
13. P.M.R. Brydon, M. Gulácsi, Phys. Rev. Lett. **96**, 036407 (2006)
14. J.K. Freericks, V. Zlatić, Rev. Mod. Phys. **75**, 1333 (2003)
15. T. Minh-Tien, Phys. Rev. B **67**, 144404(R) (2003); V.-N. Phan, M.-T. Tran, Phys. Rev. B **72**, 214418 (2006)
16. R. Lemański, Phys. Rev. B **71**, 035107 (2005)
17. P. Farkašovský, H. Čenčariková, Europ. Phys. J. B **47**, 517 (2005)
18. P.M.R. Brydon, M. Gulácsi, Phys. Rev. B **73**, 235120 (2006)
19. M. Fabrizio, A.O. Gogolin, A.A. Nersesyan, Phys. Rev. Lett. **83**, 2014 (1999)
20. C.D. Batista, A. Aliga, Phys. Rev. Lett. **92**, 246405 (2004)
21. T. Giamarchi, *Quantum Physics in One Dimension* (Oxford University Press, Oxford, 2003)
22. M. Gulácsi, Adv. Phys. **53**, 769(2004)
23. It is interesting to note that a similar effect is responsible for the ferromagnetic phases in the doped 1D Kondo lattice model [22]
24. L.I. Schiff, *Quantum Mechanics* (McGraw-Hill, New York, 1955)
25. C. Sire, Int. J. Mod. Phys. B **7**, 1551 (1993)
26. P. Farkašovský, Phys. Rev. B **60**, 10776 (1999)
27. P. Farkašovský, Phys. Rev. B **51**, 1507 (1995)
28. T. Egami, S. Ishahara, M. Tachiki, Science **261**, 1307 (1993)
29. S.R. Manmana, V. Meden, R.M. Noack, K. Schönhammer, Phys. Rev. B **70**, 155115 (2004)
30. R.E. Peierls, *Quantum Theory of Solids* (Oxford University Press, Oxford, 1955)
31. M.C. Cross, D.S. Fischer, Phys. Rev. B **19**, 402 (1979)
32. M.E. Torio, A.A. Aligia, G.I. Japaridze, B. Normand, Phys. Rev. B **73**, 115109 (2006)